APPLICATION OF DISCRETE CRACK IN NONLINEAR DYNAMIC ANALYSIS OF SHAHID RAJAEE ARCH DAM

V. Lotfi

Department of Civil Engineering , Amirkabir University, and
Mahab Ghodss Consulting Engineers, Tehran, Iran

(Received: August 3, 1998 – Accepted in Final Form: January 3, 2000)

Abstract the nonlinear discrete crack modeling of Shahid Rajaee thin arch dam is considered. The interface elements are positioned such that certain potential separated blocks can form possible failure mechanisms. The dynamic stability of theses blocks are investigated by a special finite element program "MAP-73" which its nonlinear algorithm and interface elements formulation are presented.

Key Words Arch Dams, Concrete Dams, Earthquake Engineering, Nonlinear Analysis, Discrete Crack

چکیده مدل غیرخطی ترک منفصل سد قوسی نازک شهید رجائی تحلیل شده است. المانهای میان لایه ای در موقعیتهائی تعبیه شده اند که مکانیزمهای گسیختگی برای بلوکهائی که احتمال جدائی دارند، بتوانند تشکیل گردند. پایداری دینامیکی این بلوکها بوسیله یک برنامه اجزاء محدود خاص بنام "MAP-73" مورد بررسی قرار گرفته و الگوریتم غیرخطی برنامه مذکور و روش فرمولاسیون المانهای میان لایه ای بکار رفته، ارائه شده است.

INTRODUCTION

There has been extensive research to examine the effect of contraction joints opening in the nonlinear response of arch dams [1-2]. These studies show that arch stresses reduce drastically, but cantilever stresses in the downstream face increase. For high earthquake excitations, these cantilever stresses are much higher than the tensile strength of lift surfaces, causing horizontal cracks, which grow and form separated blocks. The stability of these separated blocks for the remaining part of the excitation duration poses a major question for designers, which has not been focused in the above-mentioned literature. Although, this could be evaluated approximately by simplified rigid body blocks method [3], but it is more appropriate to model the weak horizontal surfaces by using interface elements similar to contraction joints but with greater tensile strengths.

In this paper, a special finite element program called "MAP-73" [4], and the corresponding pre- and post-processing program "MAP-P" are utilized for this purpose. The theory of the interface element formulation and the nonlinear algorithm applied are explained initially. Later, nonlinear behavior of Shahid Rajaee thin arch dam is being considered by evaluating the dynamic stability of potential separated blocks. The dam is 130m high, with the crest length of 420 m and it is being constructed in the north of Iran in the seismically active foothills of Alborz Mountain, near the city of Sari.

THEORETICAL BACKGROUND

Nonlinear static analysis is a prerequisite for a

complete nonlinear dynamic analysis, because the latter applies the results of the former as initial conditions. Therefore, it is worthwhile to concentrate initially on static analysis, although from theoretical point of view, static analysis can be considered as a special case of dynamic analysis with no inertia and damping effects.

Nonlinear Static Analysis There is much literature on the subject of nonlinear analysis [5-7]. However, it can be simply stated as an iterative process on the equation of static equilibrium

$$\underset{\sim}{K}_t \Delta \underset{\sim}{U}_{n+1}^{i+1} = \underset{\sim}{R}_{n+1} - \underset{\sim}{F}_{n+1}^{i} \quad (1)$$

in which $\underset{\sim}{K}_t$ could be taken as initial or tangent stiffness matrix leading to initial stiffness or Newton-Raphson method. The latter approach often requires much more computational time. However, there is less chance of divergence especially for large increments of loads. A more popular technique, which is a compromise between the previous two algorithms, updates the tangent stiffness matrix merely at the beginning of each increment. This is referred to as modified Newton-Raphson technique. $\underset{\sim}{R}_{n+1}, \underset{\sim}{F}^{i}_{n+1}$ denote respectively the vectors of external forces and the i^{th} estimate for the internal forces at instant $n+1$. $\Delta \underset{\sim}{U}_{n+1}^{i+1}$ is a correction which needs to be added to the previous estimate of displacements vector to yield a new improved vector of displacements as displayed below

$$\underset{\sim}{U}_{n+1}^{i+1} = \underset{\sim}{U}_{n+1}^{i} + \Delta \underset{\sim}{U}_{n+1}^{i+1} \quad (2)$$

The initial guess for vectors of displacements and internal forces at instant $n+1$ is taken as its known values for instant n.

Internal Force Vector Assuming that state of stresses in a finite element is known at some instant n, the vector of equivalent internal forces for the element is obtained by setting equal the virtual works of internal stresses and the equivalent forces, i.e.,

$$\delta \underset{\sim}{U}^T \underset{\sim}{F}_n = \int \delta \underset{\sim}{\varepsilon}^T \underset{\sim}{\sigma}_n \, dv \quad (3)$$

in which the strain vector $\underset{\sim}{\varepsilon}$ is related to displacement vector $\underset{\sim}{U}$ through matrix $\underset{\sim}{B}$.

$$\underset{\sim}{\varepsilon} = \underset{\sim}{B}\underset{\sim}{U} \quad (4)$$

By combining (3) and (4), the following relation yields

$$\delta \underset{\sim}{U}^T \underset{\sim}{F}_n = \delta \underset{\sim}{U}^T \int_v \underset{\sim}{B}^T \underset{\sim}{\sigma}_n \, dv \quad (5)$$

which must be true for an arbitrary virtual displacement. Therefore, the vector of internal forces of an element at instant n can be obtained by the following integration.

$$\underset{\sim}{F}_n = \int_v \underset{\sim}{B}^T \underset{\sim}{\sigma}_n \, dv \quad (6)$$

Tangent Stiffness Matrix The total tangent stiffness matrix is obtained by assemblage of different elemental tangent stiffness matrices which can be defined for a given discrete crack model. The nonlinearities are limited to contraction joints and some of the horizontal surfaces. It should be noted that the solid elements could be taken as usual linear isoparametric elements whose stiffness are calculated once at the beginning, assembled and stored for recursive application throughout the analysis. While the interface elements stiffness need to be updated at all iterations.

Isoparametric Interface Element The interface element is utilized to model discrete cracks and joint openings at any predefined surface. It consists of two spatial 8 noded isoparametric layers A, and B placed originally on top of each other with potential for being separated partially or completely.

The coordinates of any point on the surface of the interface element can be interpolated based on the nodal coordinates of the element.

$$x^j = \sum_{i=1}^{8} f_i \, \boldsymbol{x}_i^j \quad ; \; j = 1-3 \tag{7}$$

Similarly, the relative displacements of any point are interpolated.

$$\Delta U^j = \sum_{i=1}^{8} f_i \, \Delta \boldsymbol{U}_i^j \quad ; \; j = 1-3 \tag{8}$$

Therefore, the vector of relative displacements at any point is written as

$$\underset{\sim}{\varepsilon} = \underset{\sim}{B} \; \Delta \underset{\sim}{U} = \sum_{i=1}^{8} \underset{\sim i}{B} \; \Delta \underset{\sim}{U}_i \tag{9}$$

in which

$$\underset{\sim}{\boldsymbol{\varepsilon}}^{\boldsymbol{T}} = (\; \Delta U^1 \;\; \Delta U^2 \;\; \Delta U^3 \tag{10}$$

$$\Delta \underset{\sim i}{U}^T = (\; \Delta U_i^1 \;\; \Delta U_i^2 \;\; \Delta U_i^3 \;)$$

and $\underset{\sim i}{B}$ is a 3 x 3 diagonal matrix with each diagonal element being equal to f_i.

The local stresses at any point on the surface of the element are related to the local relative displacements in two arbitrary tangential directions and the perpendicular direction as follows

$$\underset{\sim}{\sigma}^l = \underset{\sim}{D}^l \; \underset{\sim}{\varepsilon}^l \tag{11}$$

where $\underset{\sim}{D}^l$ is a 3x3 diagonal matrix with

$$D_{jj}^l = k_j \quad ; \; j = 1-3 \tag{12}$$

k_j being the stiffness in the j^{th} direction, which is set equal to a relatively large number.

However, in case σ_3^l at a gauss point is greater than a specified limit σ^*, perfect tensile softening is assumed (i.e., k_3=0) and the element opens up. Of course, it regains its stiffness if the gauss point tries to act in compression at a later stage.

The local surfacial relative displacements vector is related to global relative displacements through matrix $\underset{\sim}{\boldsymbol{T}}$

$$\underset{\sim}{\varepsilon}^l = \underset{\sim}{T} \; \underset{\sim}{\varepsilon} = \underset{\sim}{T} \underset{\sim}{B} \Delta \underset{\sim}{U} \tag{13}$$

in which j^{th} row of matrix $\underset{\sim}{T}$ corresponds to components of a unit vector in j^{th} direction. Also, combining (9), (11) and (13) it yields:

$$\underset{\sim}{\sigma}^l = \underset{\sim}{D}^l \underset{\sim}{T} \underset{\sim}{B} \Delta \underset{\sim}{U} \tag{14}$$

Moreover, $\Delta \underset{\sim}{\boldsymbol{U}}$ can be written as

$$\Delta \underset{\sim}{U} = \underset{\sim}{G} \underset{\sim}{U} \tag{15}$$

where

$$\underset{\sim}{U}^T = (U_1^A, V_1^A, W_1^A, ..., W_8^A,$$

$$U_1^B, V_1^B, W_1^B, ..., U_8^B, V_8^B, W_8^B)$$

and

$$\underset{\sim}{G} = (-\underset{\sim}{I}, \underset{\sim}{I})$$

$\underset{\sim}{I}$ being a 24x24 identity matrix .

Finally, the stiffness matrix is obtained by setting equal internal and external virtual works of the element

$$\int_A (\delta \underset{\sim}{\varepsilon}^l)^T \underset{\sim}{\sigma}^l \, dA = \delta \underset{\sim}{U}^T \underset{\sim}{P} \tag{16}$$

Substituting (13) - (15) into (16) results in

$$\delta \underset{\sim}{U}^T \underset{\sim}{G}^T \int_A \underset{\sim}{B}^T \underset{\sim}{T}^T \underset{\sim}{D}^l \underset{\sim}{T} \underset{\sim}{B} dA \underset{\sim}{G} \underset{\sim}{U} = \delta \underset{\sim}{U}^T \underset{\sim}{P} \tag{17}$$

which must be true for arbitrary displacements vector $\delta \underset{\sim}{U}^T$. Thus the elemental equation of equilibrium is yielded.

$$\underset{\sim t}{K} \; \underset{\sim}{U} = \underset{\sim}{P} \tag{18}$$

in which

$$\underset{\sim t}{K} = \underset{\sim}{G}^T \int_A \underset{\sim}{B}^T \underset{\sim}{T}^T \underset{\sim}{D}^l \; \underset{\sim}{T} \; \underset{\sim}{B} dA \underset{\sim}{G} \tag{19}$$

The integration process is easily performed by famous gaussian procedure and $\underset{\sim t}{K}$ being the tangential stiffness matrix of the element is obtained.

Linear Dynamic Analysis It is worthwhile to explain the algorithm applied in case of linear dynamic analysis prior to the more complicated

nonlinear dynamic analysis. In the "MAP-73" program the popular Newmark method is used which is a generalization of several algorithms such as constant or linear acceleration methods. This is explained briefly below.

Consider the equation of dynamic equilibrium

$$\underset{\sim}{M}\ddot{\underset{\sim}{U}}+\underset{\sim}{C}\dot{\underset{\sim}{U}}+\underset{\sim}{K}\underset{\sim}{U}=\underset{\sim}{R} \tag{20}$$

where $\underset{\sim}{M},\underset{\sim}{C},\underset{\sim}{K}$ are mass, damping, stiffness matrices of the system respectively, and $\underset{\sim}{R}$ is vector of nodal external forces. In Newmark method, velocity and displacement vectors of instant $n+1$ are written in terms of displacement, velocity of instant n, and accelerations of instants $n, n+1$ as follows

$$\dot{\underset{\sim}{U}}_{n+1}=\dot{\underset{\sim}{U}}_{n}+\Delta t[(1-\delta)\ddot{\underset{\sim}{U}}_{n}+\delta\ddot{\underset{\sim}{U}}_{n+1}] \tag{21}$$

$$\underset{\sim}{U}_{n+1}=\underset{\sim}{U}_{n}+\dot{\underset{\sim}{U}}_{n}\Delta t+\Delta t^{2}[(\frac{1}{2}-\alpha)\ddot{\underset{\sim}{U}}_{n}+\alpha\ddot{\underset{\sim}{U}}_{n+1}] \tag{22}$$

in which δ,α are two arbitrary constants to be specified. In this report, the values of 1/2 and 1/4 are used for these constants respectively. $\underset{\sim}{U},\dot{\underset{\sim}{U}}$ and $\ddot{\underset{\sim}{U}}$ denote the vector of nodal displacement, velocity, and acceleration vectors. Solving (22) for acceleration at instant $n+1$, we obtain

$$\ddot{\underset{\sim}{U}}_{n+1}=\frac{1}{\alpha\Delta t^{2}}\overline{\underset{\sim}{U}}-\frac{1}{\alpha\Delta t}\dot{\underset{\sim}{U}}_{n}-(\frac{1}{2\alpha}-1)\ddot{\underset{\sim}{U}}_{n} \tag{23}$$

in which $\overline{\underset{\sim}{U}}$ is the difference of displacement vectors for instants n, and $n+1$. Meanwhile we can substitute (23) into (21) to get

$$\dot{\underset{\sim}{U}}_{n+1}=\frac{\delta}{\alpha\Delta t}\overline{\underset{\sim}{U}}+(1-\frac{\delta}{\alpha})\dot{\underset{\sim}{U}}_{n}+(1-\frac{\delta}{2\alpha})\Delta t\ddot{\underset{\sim}{U}}_{n} \tag{24}$$

For simplicity, (23) and (24) can be written as

$$\ddot{\underset{\sim}{U}}_{n+1}=a_{0}\overline{\underset{\sim}{U}}-a_{2}\dot{\underset{\sim}{U}}_{n}-a_{3}\ddot{\underset{\sim}{U}}_{n} \tag{25}$$

$$\dot{\underset{\sim}{U}}_{n+1}=a_{1}\overline{\underset{\sim}{U}}-a_{4}\dot{\underset{\sim}{U}}_{n}-a_{5}\ddot{\underset{\sim}{U}}_{n} \tag{26}$$

where

$$a_{0}=\frac{1}{\alpha\Delta t^{2}}\ ,\ a_{2}=\frac{1}{\alpha\Delta t}\ ,\ a_{3}=(\frac{1}{2\alpha}-1)$$

$$a_{1}=\frac{\delta}{\alpha\Delta t}\ ,\ a_{4}=(\frac{\delta}{\alpha}-1)\ ,\ a_{5}=(\frac{\delta}{2\alpha}-1)\Delta t$$

Finally, replacing (25), (26) into (20) yields

$$\hat{\underset{\sim}{K}}\underset{\sim}{U}_{n+1}=\hat{\underset{\sim}{R}}_{n+1} \tag{27}$$

in which

$$\hat{\underset{\sim}{K}}=\underset{\sim}{K}+a_{0}\underset{\sim}{M}+a_{1}\underset{\sim}{C} \tag{28}$$

$$\hat{\underset{\sim}{R}}_{n+1}=\underset{\sim}{R}_{n+1}+\underset{\sim}{M}(a_{0}\underset{\sim}{U}_{n}+a_{2}\dot{\underset{\sim}{U}}_{n}+a_{3}\ddot{\underset{\sim}{U}}_{n})+\underset{\sim}{C}(a_{1}\underset{\sim}{U}_{n}+a_{4}\dot{\underset{\sim}{U}}_{n}+a_{5}\ddot{\underset{\sim}{U}}_{n}) \tag{29}$$

$\hat{\underset{\sim}{K}}$ and $\hat{\underset{\sim}{R}}_{n+1}$ are referred to as the effective stiffness matrix, and the effective nodal force vector at instant $n+1$ respectively. Therefore, we solve for displacements at each step in (27), and substitute into (25), (26) to obtain the acceleration and velocity at instant $n+1$.

Damping Effect As mentioned in previous section, direct integration method in time is being employed for dynamic analysis. In this method, the damping matrix requires to be explicitly defined. It is customary to apply the Rayleigh damping in which the damping matrix is defined proportional to mass and stiffness matrix,

$$\underset{\sim}{C}=\alpha_{0}\underset{\sim}{M}+\alpha_{1}\underset{\sim}{K}$$

where α_{0} and α_{1} are arbitrary constants to be specified. In the analysis carried out, these were determined such that the equivalent damping for frequencies close to the first and sixth modes of vibration would be 12% of the critical damping.

Dam Reservoir Interaction There is several procedures to consider the effect of hydrodynamic pressures induced by dam-reservoir interaction,

e.g., methods based on compressible or incompressible water theories in frequency or time domain. In this paper, a conservative and computationally efficient modified Westergaard approach is employed which is explained below.

The method assumes that hydrodynamic pressures in excess of hydrostatic pressures acting on the dam body are proportional to the normal acceleration of the dam upstream surface, i.e.;

$$P = -\alpha a_n = -\frac{7}{8}\rho\sqrt{h'(h-z)}\,a_n \tag{30}$$

in which ρ, h are water density and maximum depth. h' is the depth of water at the location being considered. The normal displacement and acceleration of the dam upstream face can be defined in terms of displacements and accelerations in Cartesian coordinates system.

$$u_n = (n_x\ n_y\ n_z)\begin{pmatrix} u \\ v \\ w \end{pmatrix} \tag{31}$$

$$a_n = (n_x\ n_y\ n_z)\begin{pmatrix} \ddot{u} \\ \ddot{v} \\ \ddot{w} \end{pmatrix} \tag{32}$$

where n_x, n_y, n_z are the components of a unit vector normal to the dam upstream face outward the fluid domain. The displacements and accelerations can be interpolated by the nodal quantities.

$$\begin{pmatrix} u \\ v \\ w \end{pmatrix} = \underset{\sim}{Q}\,\underset{\sim}{U} \tag{33}$$

$$\begin{pmatrix} \ddot{u} \\ \ddot{v} \\ \ddot{w} \end{pmatrix} = \underset{\sim}{Q}\,\ddot{\underset{\sim}{U}} \tag{34}$$

Let us now convert the effect of hydrodynamic pressures into equivalent nodal forces. Setting equal the virtual works of the hydrodynamic pressures and the equivalent forces can achieve this

$$\int_A \delta \underset{\sim n}{u}^T P dA = \delta \underset{\sim}{U}^T \underset{\sim H}{R} \tag{35}$$

in which $\underset{\sim H}{\boldsymbol{R}}$ is the equivalent nodal force. Utilizing (30) - (34), then (35) can be written as

$$-\delta \underset{\sim}{U}^T \int_A \underset{\sim}{Q}^T \underset{\sim}{T}\underset{\sim}{Q}\alpha dA\,\ddot{\underset{\sim}{U}} = \delta \underset{\sim}{U}^T \underset{\sim H}{R} \tag{36}$$

where

$$\underset{\sim}{T} = \begin{pmatrix} n_x^2 & n_x n_y & n_x n_z \\ n_x n_y & n_y^2 & n_y n_z \\ n_x n_z & n_y n_z & n_z^2 \end{pmatrix}$$

Knowing that (36) must be true for an arbitrary virtual displacement, we obtain

$$-\underset{\sim}{M}_a\,\ddot{\underset{\sim}{U}} = \underset{\sim H}{R} \tag{37}$$

$$\underset{\sim}{M}_a = \int_A \underset{\sim}{Q}^T \underset{\sim}{T}\underset{\sim}{Q}\alpha dA \tag{38}$$

$\underset{\sim}{M}_a$ is the added mass matrix, which is combined with the usual mass matrix of corresponding dam finite element. In this approach, the effect of dam-reservoir interaction is considered in an efficient and conservative manner.

Nonlinear Dynamic Analysis In this section, the Newmark method explained for linear dynamic analysis is generalized to the case of nonlinear dynamic analysis.

Consider the equation of dynamic equilibrium at instant $n+1$

$$\underset{\sim}{M}\,\ddot{\underset{\sim}{U}}_{n+1} + \underset{\sim}{C}\,\dot{\underset{\sim}{U}}_{n+1} + \underset{\sim n+1}{F} = \underset{\sim n+1}{R} \tag{39}$$

where $\underset{\sim n+1}{F}$ is the vector of nodal forces equivalent to internal stresses. Based on (25) and (26) the i^{th} estimation in the iterative process for acceleration and velocity vectors are

$$\ddot{\underset{\sim n+1}{U}}^{i+1} = a_0 \underset{\sim}{\overline{U}}^{i+1} - a_2 \dot{\underset{\sim n}{U}} - a_3 \ddot{\underset{\sim n}{U}} \tag{40}$$

$$\dot{\underset{\sim}{U}}^{i+1}_{n+1} = a_1 \overline{\underset{\sim}{U}}^{i+1} - a_4 \dot{\underset{\sim}{U}}_n - a_5 \ddot{\underset{\sim}{U}}_n \quad (41)$$

where

$$\overline{\underset{\sim}{U}}^{i+1} = \overline{\underset{\sim}{U}}^{i} + \Delta \underset{\sim}{U}^{i+1} \quad (42)$$

$\overline{\underset{\sim}{U}}^{i}$ and $\overline{\underset{\sim}{U}}^{i+1}$ are respectively the i^{th}, $(i+1)^{th}$ estimates for the difference of displacement vectors at instants n, and $n+1$. Meanwhile, $\Delta \underset{\sim}{\boldsymbol{U}}^{i+1}$ is the correction, which needs to be determined at each iteration of certain incremental step. Furthermore, a good estimate for the vector of equivalent internal stresses is

$$\underset{\sim}{F}^{i+1}_{n+1} \cong \underset{\sim}{F}^{i}_{n+1} + \underset{\sim}{K}_t \, \Delta \underset{\sim}{U}^{i+1} \quad (43)$$

in which $\underset{\sim}{K}_t$ is the tangential stiffness matrix of the system. Applying (42) into (40) and (41) results in

$$\ddot{\underset{\sim}{U}}^{i+1}_{n+1} = a_0 \Delta \underset{\sim}{U}^{i+1} + \ddot{\underset{\sim}{U}}^{i}_{n+1} \quad (44)$$

$$\dot{\underset{\sim}{U}}^{i+1}_{n+1} = a_1 \Delta \underset{\sim}{U}^{i+1} + \dot{\underset{\sim}{U}}^{i}_{n+1} \quad (45)$$

where

$$\ddot{\underset{\sim}{U}}^{i}_{n+1} = a_0 \overline{\underset{\sim}{U}}^{i} - a_2 \dot{\underset{\sim}{U}}_n - a_3 \ddot{\underset{\sim}{U}}_n \quad (46)$$

$$\dot{\underset{\sim}{U}}^{i}_{n} = a_1 \overline{\underset{\sim}{U}}^{i} - a_4 \dot{\underset{\sim}{U}}_n - a_5 \ddot{\underset{\sim}{U}}_n \quad (47)$$

substituting (43) - (45) into (39) yields

$$(\underset{\sim}{K}_t + a_0 \underset{\sim}{M} + a_1 \underset{\sim}{C}) \Delta \underset{\sim}{U}^{i+1} = \underset{\sim}{R}_{n+1} - \underset{\sim}{F}^{i}_{n+1} - \underset{\sim}{M} \ddot{\underset{\sim}{U}}^{i}_{n+1} - \underset{\sim}{C} \dot{\underset{\sim}{U}}^{i}_{n+1} \quad (48)$$

based on (48), the $(i+1)^{th}$ correction for displacements vector is obtained, and using (44), (45), better estimates for acceleration and velocity vectors can be calculated.

This process recurs until convergence is achieved, having in mind that $\underset{\sim}{F}^{i}_{n+1}$ needs to be defined based on correct stresses at all iterations. It should be noted that the initial guess for vectors of acceleration, velocity, and forces equivalent to internal stresses at instant $n+1$ could be chosen as follows:

$$\ddot{\underset{\sim}{U}}^{0}_{n+1} = -a_2 \dot{\underset{\sim}{U}}_n - a_3 \ddot{\underset{\sim}{U}}_n \quad (49)$$

$$\dot{\underset{\sim}{U}}^{0}_{n+1} = -a_4 \dot{\underset{\sim}{U}}_n - a_5 \ddot{\underset{\sim}{U}}_n \quad (50)$$

$$\underset{\sim}{F}^{0}_{n+1} = \underset{\sim}{F}_n \quad (51)$$

Specialization for Linear Analysis As explained, linear dynamic analysis can be considered a special case of nonlinear dynamic analysis for which at each increment only one iteration is performed. In this manner, replacing (49) - (51) into (48), we obtain

$$\underset{\sim}{\hat{K}} \Delta \underset{\sim}{U}^{1} = \underset{\sim}{R}_{n+1} - \underset{\sim}{F}_n + \underset{\sim}{M}(a_2 \dot{\underset{\sim}{U}}_n + a_3 \ddot{\underset{\sim}{U}}_n) + \underset{\sim}{C}(a_4 \dot{\underset{\sim}{U}}_n + a_5 \ddot{\underset{\sim}{U}}_n) \quad (52)$$

in which $\underset{\sim}{\hat{K}} = \underset{\sim}{K}_t + a_0 \underset{\sim}{M} + a_1 \underset{\sim}{C}$

Noting that in linear analysis, $\underset{\sim}{\hat{K}}$ is constant and the vector of equivalent internal forces can be written in terms of displacements vector

$$\underset{\sim}{F}_n = \underset{\sim}{K} \, \underset{\sim}{U}_n$$

Equation (52) can conduce to the following relation

$$\underset{\sim}{\hat{K}} \Delta \underset{\sim}{U} = \underset{\sim}{R}_{n+1} - \underset{\sim}{\hat{K}} \underset{\sim}{U}_n + \underset{\sim}{M}(a_0 \underset{\sim}{U}_n + a_2 \dot{\underset{\sim}{U}}_n + a_3 \ddot{\underset{\sim}{U}}_n) + \underset{\sim}{C}(a_1 \underset{\sim}{U}_n + a_4 \dot{\underset{\sim}{U}}_n + a_5 \ddot{\underset{\sim}{U}}_n) \quad (53)$$

or

$$\underset{\sim}{\hat{K}} \, \underset{\sim}{U}_{n+1} = \underset{\sim}{\hat{R}}_{n+1} \quad (54)$$

where

$$\underset{\sim}{\hat{R}}_{n+1} = \underset{\sim}{R}_{n+1} + \underset{\sim}{M}(a_0 \underset{\sim}{U}_n + a_2 \dot{\underset{\sim}{U}}_n + a_3 \ddot{\underset{\sim}{U}}_n) + \underset{\sim}{C}(a_1 \underset{\sim}{U}_n + a_4 \dot{\underset{\sim}{U}}_n + a_5 \ddot{\underset{\sim}{U}}_n) \quad (55)$$

which is the same as linear dynamic relations previously obtained.

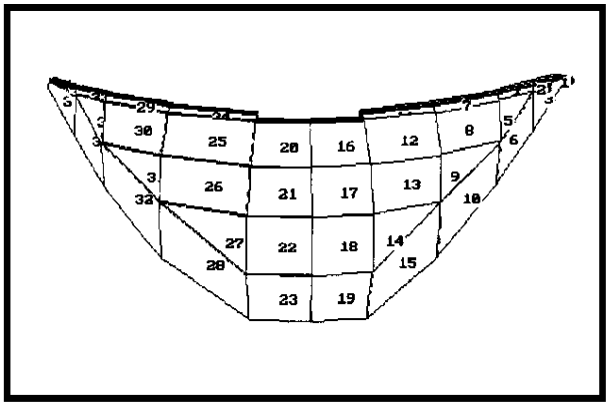

Figure 1a. Element numbers (upstream view) of Shahid Rajaee concrete arch dam model.

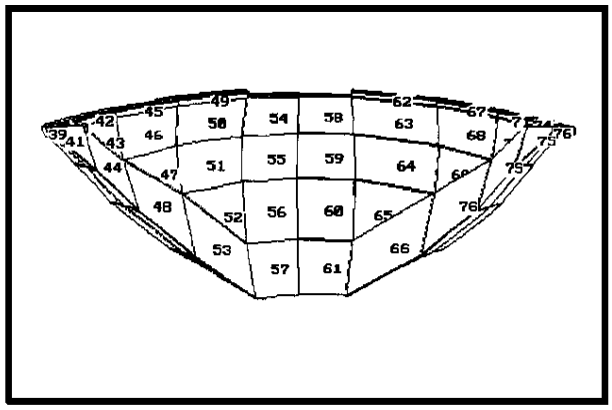

Figure 1b. Element numbers (downstream view) of Shahid Rajaee concrete arch dam model.

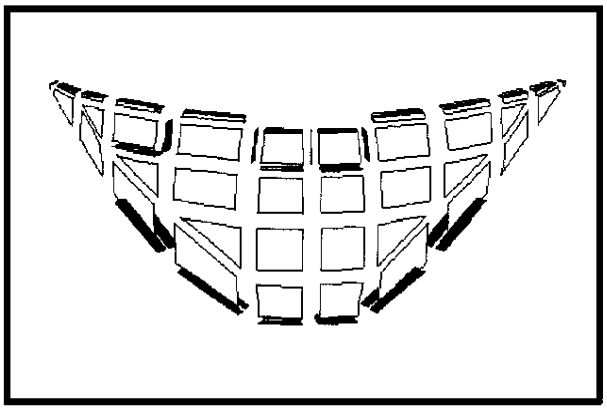

Figure 1c. Shrinked elements (20 noded solid, 16 noded interface) of nonlinear discrete crack model.

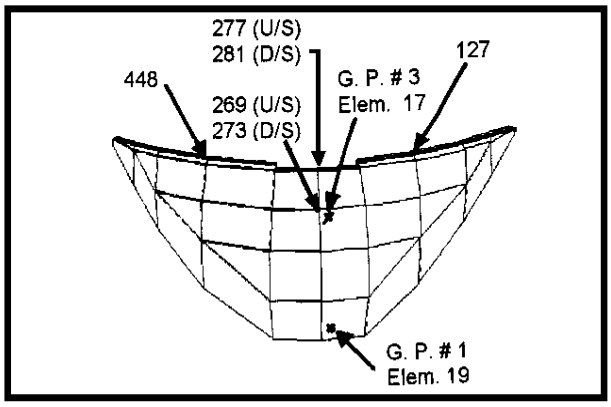

Figure 1d. Specific node numbers and stress points

FINITE ELEMENT IDEALIZATION

Selected Models Two cases are studied. Case A, a linear model used mainly for comparative purposes. Case B, a nonlinear discrete crack model in which interface elements are utilized at some predefined surfaces where cracks deemed to occur based on the linear analysis results. In both cases, the finite element mesh consists of 660 nodes and 76 isoparametric 20 noded elements (Figures 1a,b). Meanwhile in Case B, there are 26 isoparametric 16 noded interface elements to model cracks and opening of joints (Figure 1c). Although, the same number of nodes are used for both Cases of A and B, the nodes corresponding to interface elements of Case B are constrained in the linear case, to guarantee that every two nodes have similar displacements.

The foundation is also taken as rigid to keep the computational time realistic. Of course, this could influence the boundary stresses in case of linear analysis drastically. However, it is less important for nonlinear case due to joint openings at the boundaries. It should also be noted that rigid foundation assumption has less impact on stresses in the vicinity of the spillway where the major

failure mode is deemed to exist.

Basic Analysis Parameters The concrete is assumed to have the following basic characteristics:
Elastic modulus = 30.0 GPa
Poisson's ratio = 0.18
Specific weight = 24.0 kN/m^3

The interface elements, utilized for the discrete crack model (Case B) is applied with the parameters mentioned below :
Elastic modulus (Ec) = 30.0 GPa
k1=k2 (tangential stiffness) = 0.2 * Ec
k3 (normal stiffness) = 50. * Ec
σ^* (tensile stress limit for contraction joints and boundaries) = 1.5 Mpa.
σ^* (tensile stress limit for horizontal lift joints) = 3.0 Mpa.

The water is taken as incompressible, inviscid fluid, with weight density of 10.0 kN/m^3 and the water level to be at elevation 485.0 m.a.s.l (h=122.0 m)

Static and Dynamic Loading It should be mentioned that static loads (weight , hydrostatic pressures) are visualized as being incrementally increasing in time until they reach their full magnitude. Therefore the same time step of 0.01 second, which is chosen in dynamic analysis, is also considered as time increment of static loads application. It should be noted that time for static analysis is just a convenient tool for applying the load incrementally, but it is obvious that inertia and damping effects are disregarded in the process. In this respect, the dead load is applied in one increment and hydrostatic pressures thereafter in nine increments at negative range of time. At time zero, the actual nonlinear dynamic analysis begins with the static displacements and stresses being applied as initial conditions.

The dynamic excitations include the three components of Friuli-Tolmezzo earthquake records normalized on the basis of frequency content for MDE condition with a peak ground acceleration of 0.42g. It needs to be mentioned that even though time duration of 20 seconds was applied on the initial trial cases, it was noticed that the response declines drastically after 6.0 seconds. For this reason and due to long execution times, the time duration was limited to 6.0 seconds in the main analyses carried out.

ANALYSIS RESULTS

As mentioned in previous section, two models are considered , the linear model (Case A) and, the nonlinear discrete crack model (Case B). These cases are analyzed and the results are displayed in the following forms.

- Snapshots of the state of stresses on deformed shape together with contour of one of the principal stresses at specific instants of time.
- History of displacements for few nodes

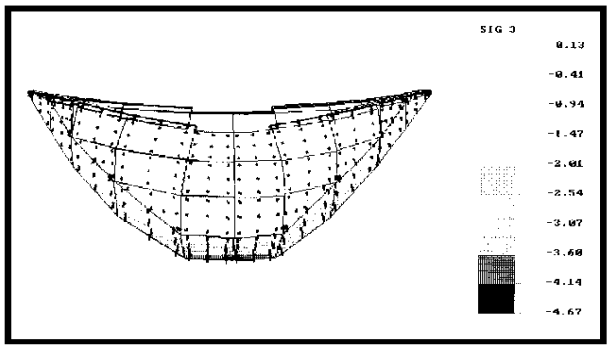

Figure 2a. Maximum compressive principal stresses (MPa.) of linear model (case A) at time – 0.09 sec.

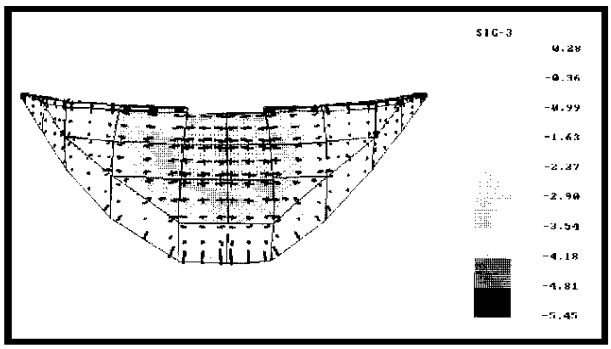

Figure 2b. Maximum compressive principal stresses (MPa.) of linear model (case A) at time 0.0 sec.

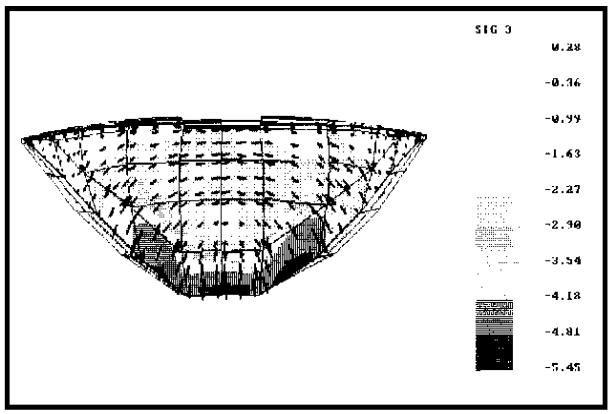

Figure 3a. Maximum compressive principal stresses (MPa.) of linear model (case A) at time 0.0 sec.

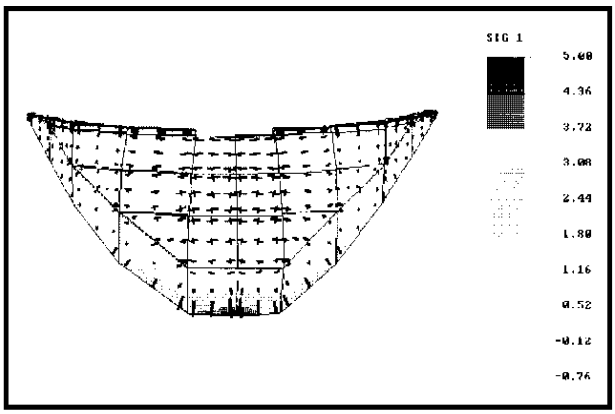

Figure 3b. Maximum tensile principal stresses (MPa.) of linear model (case A) at time 0.0 sec.

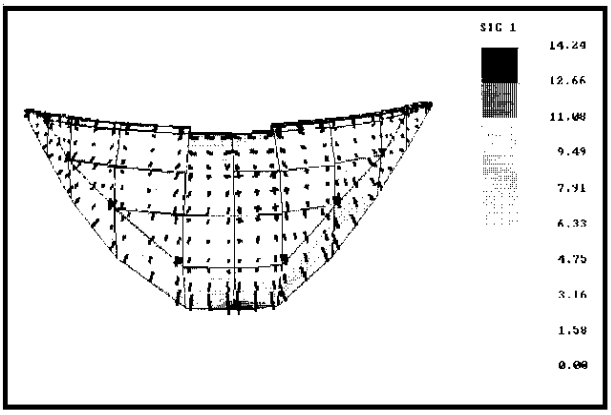

Figure 4a. Envelope of maximum tensile principal stresses (MPa.) for linear model (case A).

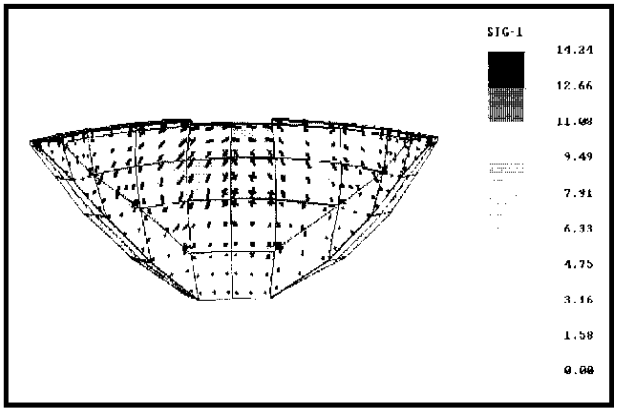

Figure 4b. Envelope of maximum tensile principal stresses (MPa.) for linear model (case A).

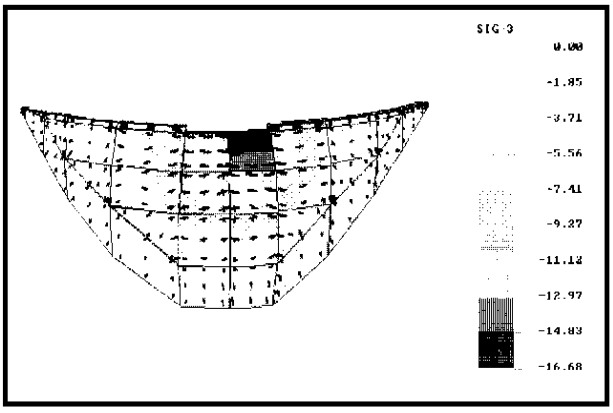

Figure 5a. Envelope of maximum compressive principal stresses (MPa.) for linear model (case A).

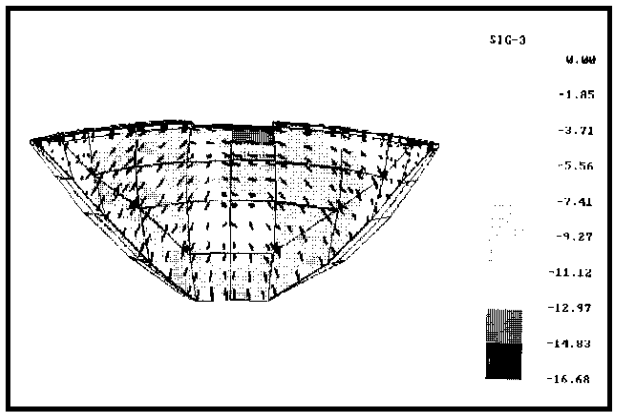

Figure 5b. Envelope of maximum compressive principal stresses (MPa.) for linear model (case A).

TABLE 1. Maximum Principal Stresses (MPa.) for Linear Model (A).

Location	σ_1		σ_3	
	U/S	D/S	U/S	D/S
Spillway	7.9	7.9	-16.7	-14.8
Base and Abutments	14.2	3.1	-9.2	-13.0

TABLE 2. Maximum Displacements (Cm) at Dam Crest for Linear Model (A)

Component	Displacements of Dam Crest		
	Left 1/4 point	Center point	Right 1/4 point
U(cross-canyon)	+3.0	-1.6	-4.6
V(stream)	+4.2	+11.0	+8.0
W(vertical)	-0.4	-1.4	+0.6

TABLE 3. Maximum Principal Stresses (MPa.) for Nonlinear Discrete Crack Model (B).

Location	σ_1		σ_3	
	U/S	D/S	U/S	D/S
Spillway	5.6	6.0	-15.0	-17.6
Base and Abutments	7.5	2.0	-7.0	-13.5

TABLE 4. Maximum Displacements (Cm) at Dam Crest for Nonlinear Discrete Crack Model (B)

Component	Displacements of Dam Crest		
	Left 1/4 point	Center point	Right ¼ point
U(cross-canyon)	+4.0	-2.4	-5.3
V(stream)	+6.4	+12.0	+9.4
W(vertical)	+0.8	+2.1	+1.3

specified on Figure 1d.

- History of stress components or principal stresses for few elements at certain Gauss points specified on Figure 1d.
- History of horizontal or vertical joint openings (Figure 1c) crossing the nodes shown on Figure 1d in case of nonlinear discrete crack model (Case B).
- Contour of the envelope of maximum principal tensile or compressive stresses occurring throughout the time.

Linear Analysis The linear model (Case A) is considered just as a comparative case. It is apparent that the state of stresses at the base could be significantly overestimated in this case due to rigid foundation assumption. However, it is expected to be a good representative of a more accurate flexible foundation model in the middle part of the dam.

The results of stresses for Case A are displayed on Figures 2-5, the snapshots at specific times, and the envelope of maximum principal stresses. It is

noted that due to dead weight loading (i.e., $t=-0.09\,sec$), the maximum compressive principal stress at the upstream face of the base reaches a value of $\sigma_3 = -4.67\text{MPa}$. At the end of staticloading (i.e., $t = 0.0$), the base of the dam on upstream face goes into tension ($\sigma_1 = 5.00\,\text{MPa}$), while at the downstream face (base and abutments) acts in compression ($\sigma_3 = -5.45\,\text{MPa}$). The maximum principal stresses at each face throughout the time are extracted from envelope diagrams showed on Figures 4 and 5 and they are tabulated in Table 1. It is observed that, there are very high tensile stresses occurring at the base of the dam, which is due basically to rigid foundation model deficiency, and high tensile stresses in the area of spillway, which in reality are released with opening of contraction joints.

The displacements at the left quarter point, center, and right quarter point of the dam crest are also monitored through time and the maximums are summarized in Table 2.

Nonlinear Discrete Crack Model (Case B) interface elements of discrete crack model are shown on Figure 1c. It is seen that interface elements provide two potentially separated blocks, under the spillway, and at the left quarter point. Meanwhile, the interface elements are also utilized in a major part of the boundary.

The results of the analysis are displayed in Figures 6-11. It is evident that for dead weight ($t = -0.09$ Sec.), basically the same compressive stresses as of linear case are present at the base of the dam on upstream face ($\sigma_3 = -4.63\text{MPa}$). However, when the hydrostatic load action is completed (*i.e.,* $t=0.0$), the base interface elements open up and relieve the tensile stresses induced at the upstream face of the base of the dam. This also causes an increase in compressive stresses on downstream face (i.e., $\sigma_3 = -5.81\text{MPa}$.). The maximum principal stresses throughout the execution time are tabulated in Table 3.

It is noted that in the spillway region, tensile arch stresses are released by opening of the joints but, there are still tensile stresses of lower magnitude in inclined directions. Meanwhile, the compressive stresses of the downstream face increase in comparison with the linear case . At the base of the dam and abutments, the tensile stresses are relieved up to the point that the interface elements are extended (Figure 1c). However at the corners, stress concentration are occurring ($\sigma_1 = 7.5\text{MPa}.$). Furthermore, the compressive stresses increase slightly in the downstream face while they decrease on the upstream face in comparison with the linear case.

The history of displacements at the left quarter point, center, and right quarter point at the dam crest are also monitored through time and the maximums are summarized in Table 4.

To evaluate the influence of interface elements, displacements and stress components of Cases A, and B are compared on Figures 12-14. It is noticed that for discrete crack model, the vertical component of the center point at the dam crest is influenced more due to joint openings than the stream component. The joint openings are also displayed in Figure 15 , with a maximum of 1.8 cm occurring in horizontal direction under the spillway.

SUMMARY AND CONCLUSIONS

The nonlinear behavior of Shahid Rajaee dam is considered by evaluating the dynamic stability of certain potential separated blocks. For this purpose an special finite element program "MAP-73" is utilized whose nonlinear algorithm and interface elements formulation are presented.

Two cases are considered, linear Case A , and nonlinear discrete crack model (B). In both cases, the foundation is assumed rigid to avoid very lengthy computational times. Of course, this assumption would overestimate the stresses at the boundary significantly in the linear case. However, it has less effect on the nonlinear cases.

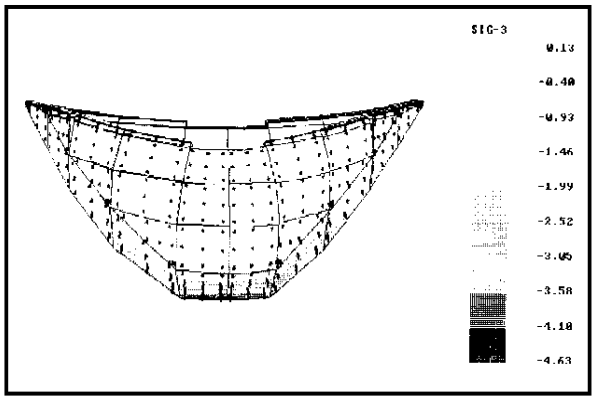

Figure 6a. Maximum compressive principal stresses (MPa.) of nonlinear discrete crack model (case B) at time – 0.09 sec.

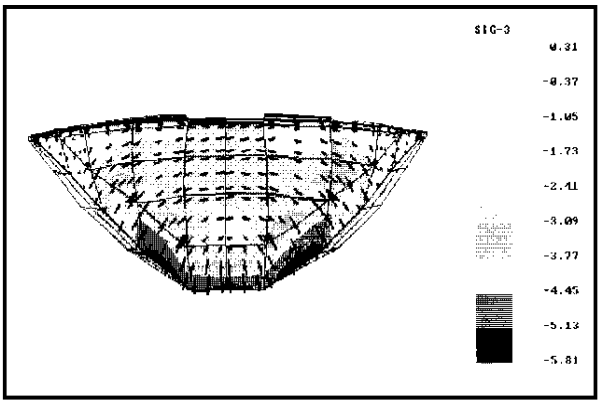

Figure 6b. Maximum compressive principal stresses (MPa.) of nonlinear discrete crack model (case B) at time 0.0 sec.

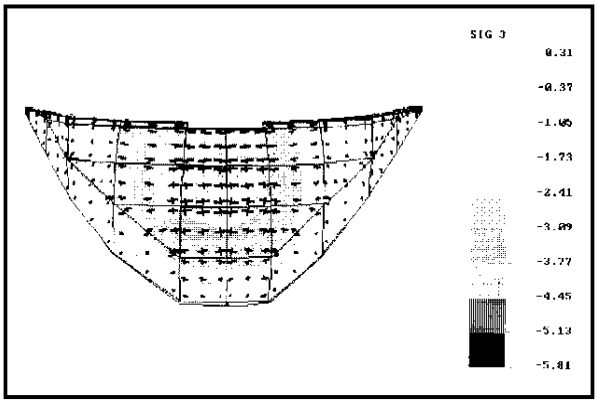

Figure 7a. Maximum compressive principal stresses (MPa.) of nonlinear discrete crack model (case B) at time 0.0 sec.

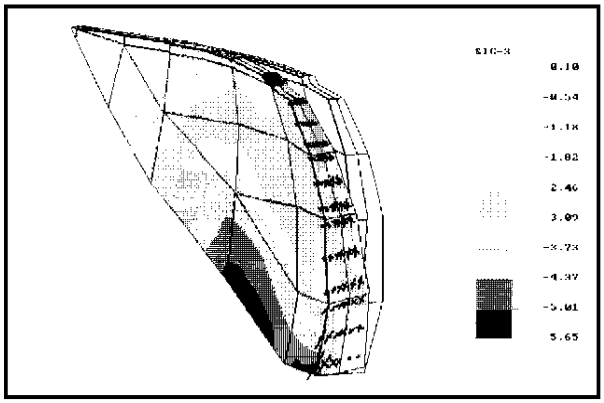

Figure 7b. Maximum compressive principal stresses (MPa.) of nonlinear discrete crack model (case B) at time 0.0 sec.

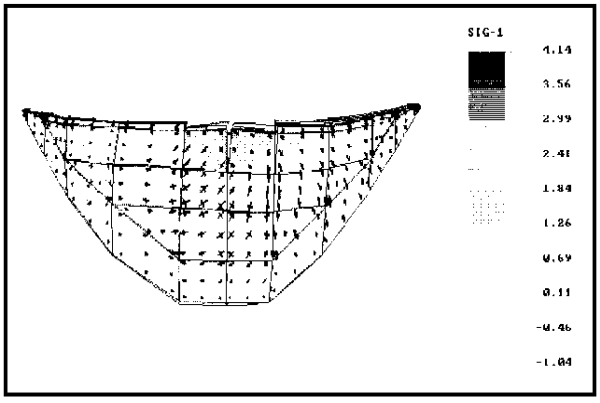

Figure 8a. Maximum tensile principal stresses (MPa.) of nonlinear discrete crack model (case B) at time 4.6 sec.

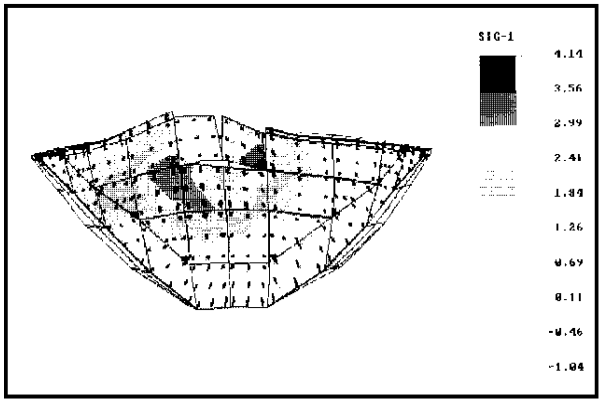

Figure 8b. Maximum tensile principal stresses (MPa.) of nonlinear discrete crack model (case B) at time 4.6 sec.

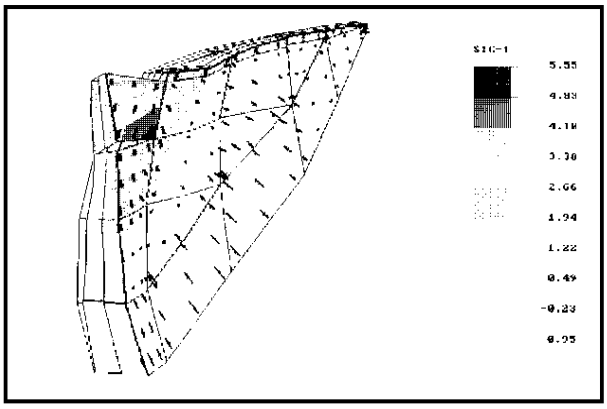

Figure 9a. Maximum tensile principal stresses (MPa.) of nonlinear discrete crack model (case B) at time 4.62 sec.

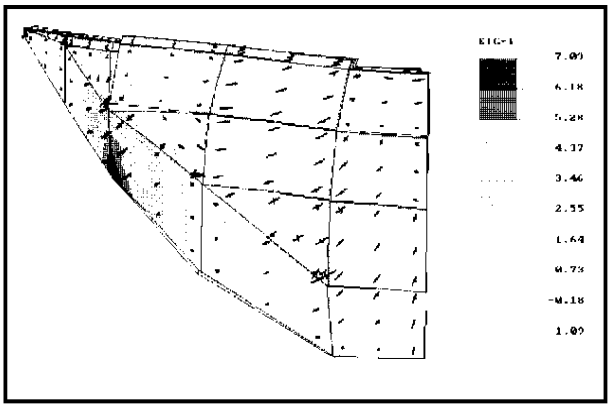

Figure 9b. Maximum tensile principal stresses (MPa.) of nonlinear discrete crack model (case B) at time 4.74 sec.

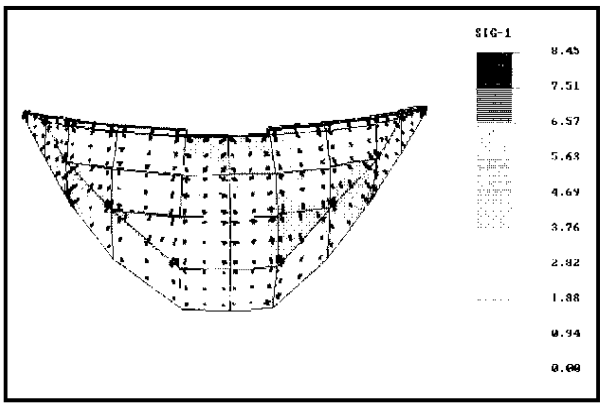

Figure 10a. Envelope of maximum tensile principal stresses (MPa.) for nonlinear discrete crack model (case B).

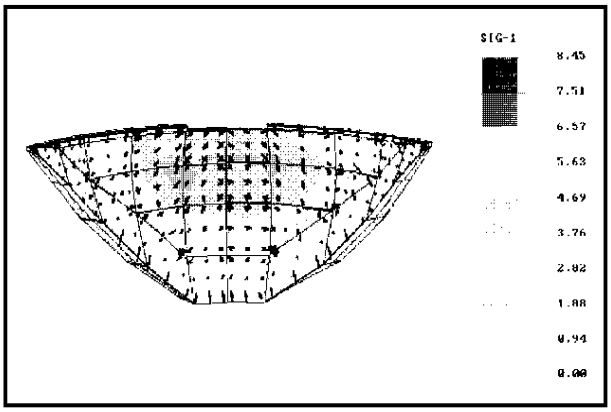

Figure 10b. Envelope of maximum tensile principal stresses (MPa.) for nonlinear discrete crack model (case B).

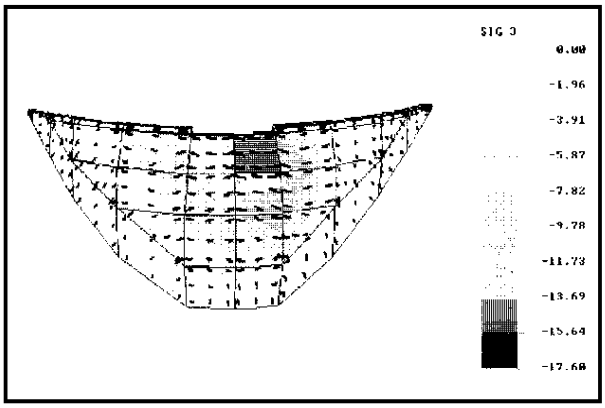

Figure 11a. Envelope of maximum compressive principal stresses (MPa.) for nonlinear discrete crack model (case B).

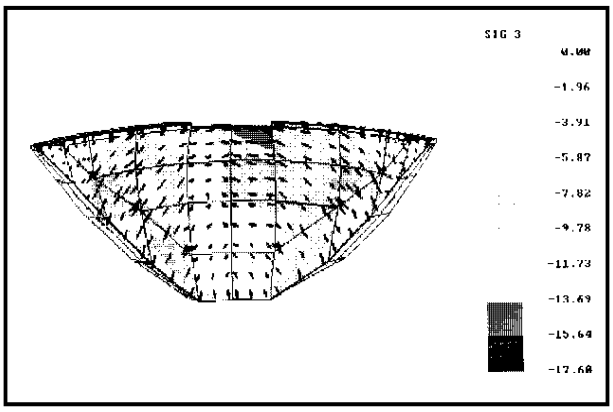

Figure 11b. Envelope of maximum compressive principal stresses (MPa.) for nonlinear discrete crack model (case B).

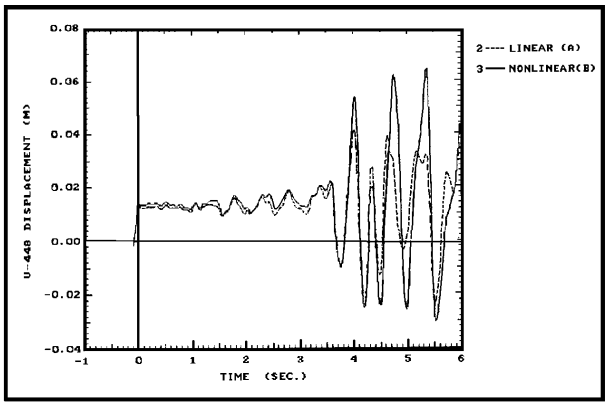

Figure 12a. Comparison of displacements in stream direction at left quarter point of dam crest.

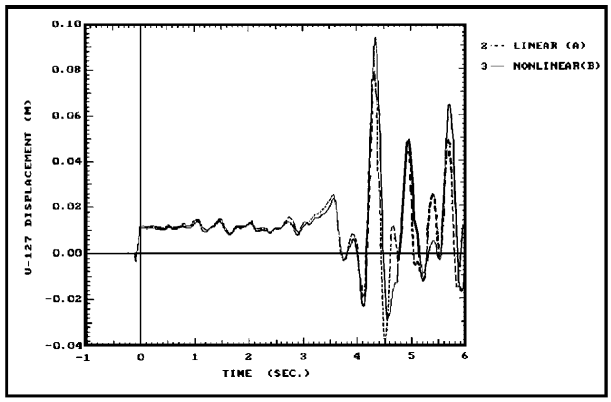

Figure. 12b. Comparison of displacements in stream direction at right quarter point of dam crest.

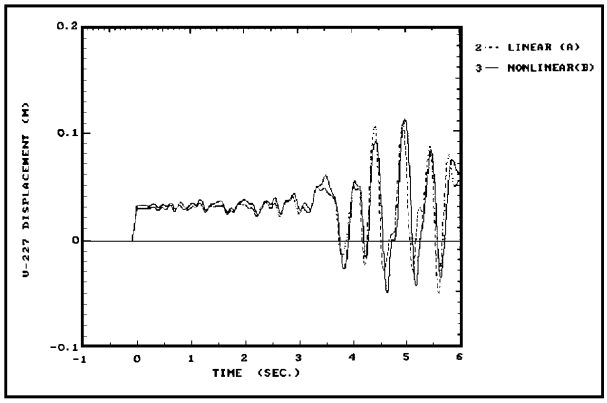

Figure 13a. Comparison of displacements in stream direction at center point of dam crest.

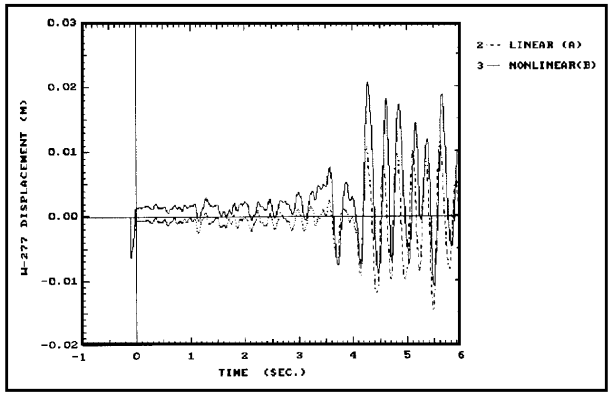

Figure 13b. Comparison of displacements in vertical direction at center point of dam crest.

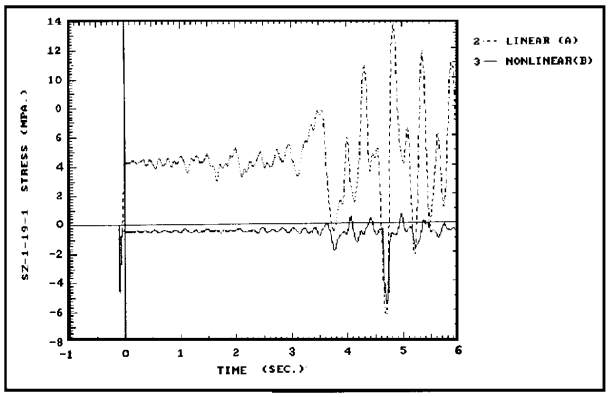

Figure 14a. Comparison of vertical stress history at upstream face of the base of the dam.

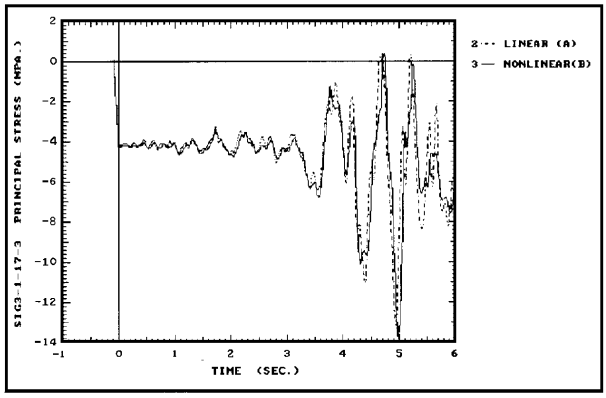

Figure 14b. Comparison of maximum compressive stress history at Gauss point No. 3 of element 17.

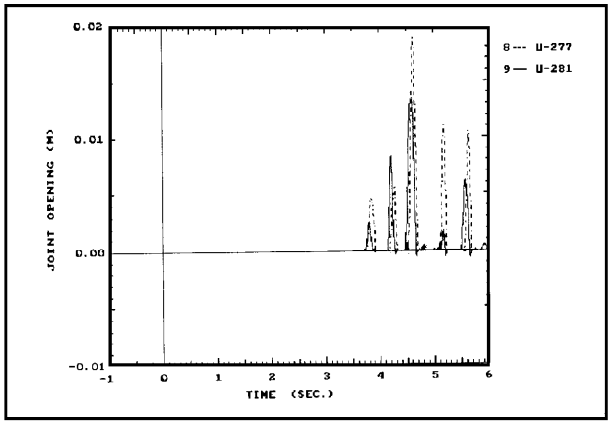

Figure 15a. Horizontal joint opening of middle blocks (upstream, and downstream face points) for nonlinear discrete crack model (case B).

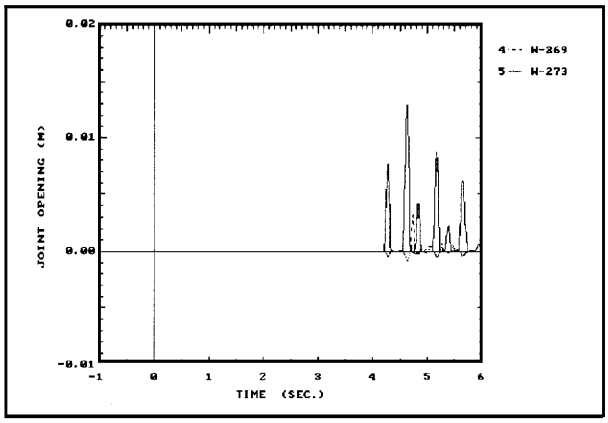

Figure 15b. Vertical joint opening of middle blocks (upstream, and downstream face points) for nonlinear discrete crack model (case B).

The cases were analyzed and discussed in previous sections. The main conclusions obtained can be listed as follows:

- There is basically the same state of stresses and deformation at the end of dead weight analysis for both cases.
- At the end of static analysis, high tensile stresses are observed in the linear case at the upstream face of the base of the dam. This is reduced to nil for the discrete crack model. At the same time, compressive stresses increase in the downstream face on the base and abutments for the nonlinear model.
- In the spillway region, tensile stresses decrease from 7.9MPa. in the case of linear model to a value of 6.0MPa. for discrete crack model. Meanwhile, the compressive stresses are increased from −16.7MPa. in linear case to −17.6MPa. for discrete crack model.
- In nonlinear model, the maximum joint opening is 1.8 Cm, displacements are increased and the dam has remained stable throughout the analysis.
- The nonlinear discrete crack model has converged with displacements, joint openings in an acceptable range. However, it seems that elasto-plastic behavior of concrete could also be significant due to high magnitude of compressive stresses present, which was neglected in this work.

REFERENCES

1. Fenves, G. L. and Mojtahedi, S., "Earthquake Response of an Arch Dam with Contraction Joint Opening", ***Dam Engineering***, Vol. 4, No. 2, (1993), 197-218.

2. Fenves, G. L., Mojtahedi, S., and Reimer, R. B., "Effect of Contraction Joints on Earthquake Response of an Arch Dam", ***Journal of Structural Eng. ASCE***, Vol. 118, (1992), 1093-1055.

3. Lotfi, V., Mokhtar-Zadeh, A., Sadeghifard, H., Arasteh, T.and Weiland, M., "Behavior of Karun I Arch Dam in Iran under the Maximum Credible Earthquake", ***Proc. Int. Symp. on Arch Dams***, Nanjing, China, (1992), 514-521.

4. Lotfi, V., "MAP-73, Mahab Ghodss and Tehran Polytechnique University Software", Mahab Ghodss Consulting Engineers, Tehran, Iran, (1994).

5. Bathe, K. J., "Finite Element Procedures in Engineering Analysis", Prentice-Hall, Inc., (1982).

6. Chen, W. F., "Plasticity in Reinforced Concrete",McGraw-Hill , (1982).

7. Owen, D. R. J., Hinton, E., "Finite Elements in Plasticity", Pine ridge Press Limited, (1980).